Colloid Polym Sci (2006) 284: 1097–1105
DOI 10.1007/s00396-006-1486-7

ORIGINAL CONTRIBUTION

Selim Kara
Önder Pekcan
Ayfer Sarac
Ertan Arda

Film formation stages for poly(vinyl acetate) latex particles: a photon transmission study

Received: 1 July 2005
Accepted: 10 March 2006
Published online: 13 April 2006

S. Kara (✉) · E. Arda
Department of Physics,
Trakya University,
22030 Edirne, Turkey
e-mail: skara@trakya.edu.tr
Tel.: +90-284-2120923
Fax: +90-284-2137053

Ö. Pekcan
Department of Physics, Isik University,
34398 Maslak, Istanbul, Turkey

A. Sarac
Department of Chemistry,
Yildiz Technical University,
34210 Esenler, Istanbul, Turkey

Abstract Photon transmission technique was used to monitor the evolution of transparency during film formation from poly(vinyl acetate) (PVAc) latex particles. The latex films were prepared below the glass transition temperature (T_g) of PVAc. These films were annealed at elevated temperatures in various time intervals above the T_g of PVAc. It is observed that transmitted photon intensity (I_{tr}) from these films increased as the annealing temperature is increased. It is seen from I_{tr} curves that there are two film formation stages. These successive stages are named void closure (viscous flow) and interdiffusion. The activation energies for viscous flow (ΔH) and backbone motion (ΔE_b) were obtained by using well-defined models. The averaged values of the backbone (ΔE_b) and the viscous flow activation energies (ΔH) were found to be 188.6 and 5.6 kcal/mol, respectively. The minimum film formation (τ_M,T_M) and healing points (τ_H,T_H) were determined. Minimum film formation (ΔE_M) and healing activation energies (ΔE_H) were measured using these time–temperature pairs. ΔE_M and ΔE_H were found to be 32.5 and 28.3 kcal/mol, respectively.

Keywords Film formation · PVAc latex · Viscous flow · Interdiffusion · Activation energy

Introduction

There are many application areas of water-borne and solvent-borne polymeric systems such as paints, paper coatings, adhesives, carpet backing and textiles [1]. All kinds of coatings are a major issue for industry, and this requires further advances in the understanding of film formation mechanism from polymer colloids. In the past few years water-based polymer latexes have gained more attention in the coating and adhesives industries over conventional solvent-based systems, mainly due to restrictions imposed by environmental requirements. Water-borne coatings offer advantages of low odor, low combustibility, quick drying and inexpensive manufacturing costs.

Aqueous or non-aqueous dispersions of colloidal particles with glass transition temperature (T_g) above the drying temperature are named hard latex dispersion; however, aqueous dispersion of colloidal particles with T_g below the drying temperature is called soft latex dispersion. The term "latex film" normally refers to a film formed from soft particles where the forces accompanying the evaporation of water are sufficient to compress and deform the particles into a transparent, void-free film [2, 3]. However, hard latex particles remain essentially discrete and undeformed during drying process. Film formation from these dispersions can occur in several stages. In both cases, the first stage corresponds to the wet initial state. Evaporation of solvent leads to a second stage in which the particles form a close packed array; here, if the particles are soft, they are deformed to polyhedrons. Hard latex, however, stays undeformed at this stage. Annealing of soft particles causes diffusion across particle–particle boundaries, which leads the film to a homogeneous continuous material. Annealing of hard latex system above the minimum film formation temperature (MFFT), deformation of particles first leads to void closure [4, 5] and then, after the voids disappear, diffusion across

particle–particle boundaries starts, i.e. the mechanical properties of hard latex films can be evolved by annealing after all solvent has evaporated and all voids have disappeared. This process is called coalescence. The mechanical properties of latex films are dependent on the molecular weight, its distribution [6, 7] and sensitive to stabilizers [8] and surfactants [9]. In addition, the quality of these films, for a given molecular weight, depends on the annealing time and annealing temperature [10–13].

After void closure process is completed, the mechanism of film formation by annealing of hard latex films is known as interdiffusion of polymer chains followed by healing at polymer–polymer interface. In general when two identical polymeric materials are brought into contact at a temperature above their glass transition temperature, the junction surface gradually disappears and becomes indistinguishable from any other surface that might be located within the bulk material. Brownian motion drives the polymer chains across the junction until eventually, all traces of the original interface are lost; at this point, we say the junction has 'healed'. Many years ago Voyutskii [14] suggested that the formation of a continuous, strong and water-impermeable film involves polymer diffusion across the junction of identical polymer particles. The molecular interpenetration of the healing process is related to the phenomenon of self-diffusion in bulk polymers, but the two are not identical. In self-diffusion, polymer coils move over distances many times their mean diameter, whereas healing is eventually complete in the time it takes a polymer coil initially next to the junction surface to move halfway across it. The 'healing time' (τ_H) can then be comparable to the configurational relaxation time (τ_e) of a polymer chain. When polymer chains are much longer than a certain length, diffusion of chains is pictured as a wormlike motion described by the reptation model proposed by de Gennes [15]. The reptation time (T_r) gives the time necessary for a polymer to diffuse a sufficient distance for all memory of the initial tube to be lost. Prager and Tirrell [16] derived a relation for the crossing density of the chains by using the reptation model during the healing process. Wool and O'Connor [17] employed reptation to study crack healing in terms of several stages, including wetting, diffusion and randomization, where at the end of the wetting stage, potential barriers associated with the inhomogeneties at the interface disappear, and chains are free to move across the interface by a randomization process.

Film formation from latex particles was studied using several experimental techniques within the last decade. Transmission electron microscopy (TEM) has been used to examine the morphology of dried latex films [18, 19]. Small-angle neutron scattering (SANS) was used to examine deuterated particles in a protonated matrix. It was observed that the radius of the deuterated particle increased in time as the film was annealed [20] and as the polymer molecules diffused out of the space to which they were originally confined. Polymer diffusion has also been studied using fluorescence measurements [21] in conjunction with latex particles labelled with donor and acceptor chromophores. Steady-state fluorescence (SSF) method was also used for studying film formation from hard latex particles [22, 23]. Recently, we have performed various experiments with photon transmission method using UV-visible (UVV) spectrophotometer to study latex film formation from polymethylmethacrylate (PMMA) and polystyrene (PS) latexes, where void closure and interdiffusion processes at the junction surfaces are studied [24–28]. These studies all indicate that the annealing leads to polymer diffusion and mixing as the particle junction heals during latex film formation.

In this work, film formation from low-T_g, poly(vinyl acetate) (PVAc) latex particles was studied by using photon transmission technique. Various stages of film formation were generated by annealing the dried latex films at equal time intervals above the glass transition temperature (T_g) of PVAc. Transmitted light intensities, I_{tr} were measured by using a UVV spectrophotometer. The increase in I_{tr} intensity by increasing annealing temperature was explained by the successive stages of film formation, which are called void closure, healing and interdiffusion processes. Minimum film formation (τ_M,T_M) and healing points (τ_H,T_H) were determined. The activation energies of the minimum film formation and healing at the particle–particle junction were obtained using these time–temperature pairs. Void closure equation was derived below (τ_H, T_H), and the activation energy of viscous flow was measured. The model developed by Prager and Tirrell (PT) was used to explain the behaviour of I_{tr} on the point (τ_H,T_H), and then the backbone activation energy of interdiffusing polymer chains was obtained.

Experimental

Preparation and properties of PVAc latex particles

An Elsan Fibre Co. (Turkey) VAc monomer inhibited with 15 ppm *p*-hydroquinone was used at commercial purification. Boysan Co. (Turkey) 88 % hydrolyzed polyvinyl alcohol (PVOH) (17-88) was used as protective colloid. Ethoxylated nonylphenol (NP 30; 30 mol) product of the Turkish-Henkel Chemicals Industry Co. (Turkey) was used to achieve the stability of the latexes. Merck ammonium persulfate was used as received as an initiator. Nopco-1497 was used as an antifoam agent. Merck sodium bicarbonate ($NaHCO_3$) was used as a buffer to keep the pH of the reaction medium between 4.5 and 5.5. Deionized water was used in the polymerization.

Polymerization was performed in a 1-l glass emulsion polymerization reactor equipped with a mechanical stirrer having a constant speed of 200 rpm and a reflux condenser in a total batch period of 3 h. Only 10 % of the total VAc monomer was introduced at the beginning of the reaction at

60 °C, and the remaining monomer was added dropwise at 71±2 °C from dropping funnels during the remaining time. An ammonium persulfate initiator was dissolved in a small amount of water, and these freshly prepared initiator portions were added at 30-min intervals throughout the reaction. VAc emulsion homopolymerization was carried out under atmospheric conditions according to the recipe shown in Table 1.

Polymer conversion was monitored gravimetrically. The viscosity of the latex was determined as 22.5 cP by a Brookfield Programmable DV-II model viscometer with spindle number 4 at 25 °C after diluting 40 % (wt.) solid content of sample. The weight average molecular weight $(\overline{M}_w)$ of polymer was determined by the GPC Agilent model 1100 type instrument with a refractive index detector and calibrated with PS standarts consisting of three Waters styragel columns (HR 4, HR 3 and HR 2). $\overline{M}_w$ of the PVAc homopolymer was found (171,875 g/mol). Glass transition temperature (T_g) of homopolymer was determined by using DSC Mettler Toledo model 822 type and found to be 18.7 °C. The particle size of the latex was determined by Malvern Zetasizer Nano ZS model instrument. The average size of the PVAc particles was found to be 735.2 nm.

Film preparation and photon transmission measurements

Latex film preparation was carried out in the following manner. PVAc latex particles were dispersed in water in a test tube as 2 % (w/v) solid content. Five latex films were produced from this dispersion by placing the same number of drops on a glass plate (1.2×2.2 cm^2 in size) and allowing the water to evaporate at 13 °C under the T_g of PVAc. Here, we were careful to ensure that the liquid dispersion from the droplets covers the whole surface area of the plates and remains there until the water has evaporated. Samples were weighed before and after film casting to determine the film thicknesses. The average film thickness is measured as 23.87 μm.

Table 1 Recipe used in homopolymerization experiment

Substance	Weight (%)
VAc	43.71
PVOH	1.88
NP 30	3.60
Initiator	0.24
$NaHCO_3$	0.12
Nopco-1497	0.08
Water	50.37
Total	100.00

The annealing processes of the latex films were performed in an oven in air above T_g of PVAc after the evaporation of water in 1-, 2.5-, 5-, 10- and 15-min time intervals at elevated temperatures from 25 to 100 °C. The temperature was maintained within ±0.5 °C during annealing. After each annealing step transmitted photon intensity, I_{tr}, on the film samples was detected between 350 and 450 nm by a UVV spectrophotometer (Lambda 2S of PerkinElmer, USA) at room temperature. A glass plate was used as a standard for all UVV experiments. Errors in UVV measurements originate mostly from the surface inhomogeneities (voids and cracks) of film samples, which cause variation in I_{tr} intensities. The noise-to-signal ratio in I_{tr} is quite low (1–2 %) and can be neglected in error estimations.

Results and discussion

Transmitted photon intensities, I_{tr}, at 350 nm from latex films vs annealing temperature for the samples annealed at 1-, 2.5-, 5-, 10- and 15-min time intervals are shown in Fig. 1. Data in Fig. 1 all indicate that films become transparent as they are annealed. In other words films scattered less light due to homogenization during film formation. All the curves in Fig. 1 have the same characteristic behavior. At the beginning of annealing process I_{tr} curves increase slowly (stage I). Increasing the annealing temperature, I_{tr} curves increase drastically (stage II) and then reach a plateau. The increase in I_{tr} may be interpreted by the mechanisms of void closure, healing and interdiffusion processes. Spherical particles that have increasing surface energy flow to intervoids (void closure) at the early stage of annealing (stage I), where the radius of interparticle voids becomes smaller and film surface becomes more homogeneous; consequently, transparency of film starts to increase. If the annealing is carried on, chain segments (minor chains) move across the particle–particle interfaces, and therefore, latex film becomes more transparent. This process is called healing. At high annealing temperatures the chains gain sufficient kinetic energy to transform its centre of mass across the junction surface (interdiffusion) (stage II), and therefore, latex film becomes fully transparent.

Schematic figure of film formation from latex particles and their relationship with the mean free and optical paths (<l> and *s*) of a photon are presented in Fig. 2. The early stage of film formation is shown in Fig. 2a, where close-packed particles form a powder film which includes many voids. This film yields low I_{tr} and high I_{sc} values due to short<l> and *s* lengths. Figure 2b presents a film where, due to annealing, interparticle voids start to disappear, giving rise to higher<l> and the longest *s* values. In such a film, one can observe higher I_{tr} intensities. Finally, Fig. 2c shows a fully transparent film with the longest<l> but

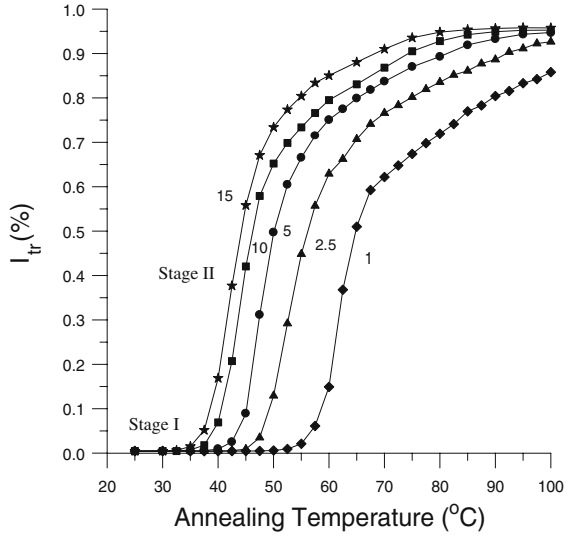

Fig. 1 Plot of I_{tr} vs annealing temperature for the films annealed at 1-, 2.5-, 5-, 10- and 15-min time intervals

smaller s values. This film should present highest I_{tr} intensities as contrary to I_{sc} intensities.

Particle deformation and void closure

To quantify the behaviour of I_{tr} at the first step of annealing, we introduce the phenomenological void closure model. The void closure kinetics can determine the time for optical transparency and latex film formation. To relate the shrinkage of spherical void of radius, r, to the viscosity of surrounding medium, η, an expression was derived and given by the following relation [29]:

$$\frac{dr}{dt} = -\frac{\gamma}{2\eta}\left(\frac{1}{\rho(r)}\right), \tag{1}$$

where γ is surface energy, t is time and $\rho(r)$ is the relative density. It has to be noted that here, surface energy causes a decrease in void size, and the term $\rho(r)$ varies with the microstructural characteristics of the material such as the number of voids, the initial particle size and packing. Equation 1 is similar to one, which was used to explain the time dependence of the MFFT during latex film formation [5, 30]. If the viscosity is constant in time, integration of Eq. 1 gives the relation as

$$t = -\frac{2\eta}{\gamma}\int_{r_0}^{r}\rho(r)dr, \tag{2}$$

where r_0 is the initial void radius at time t=0.

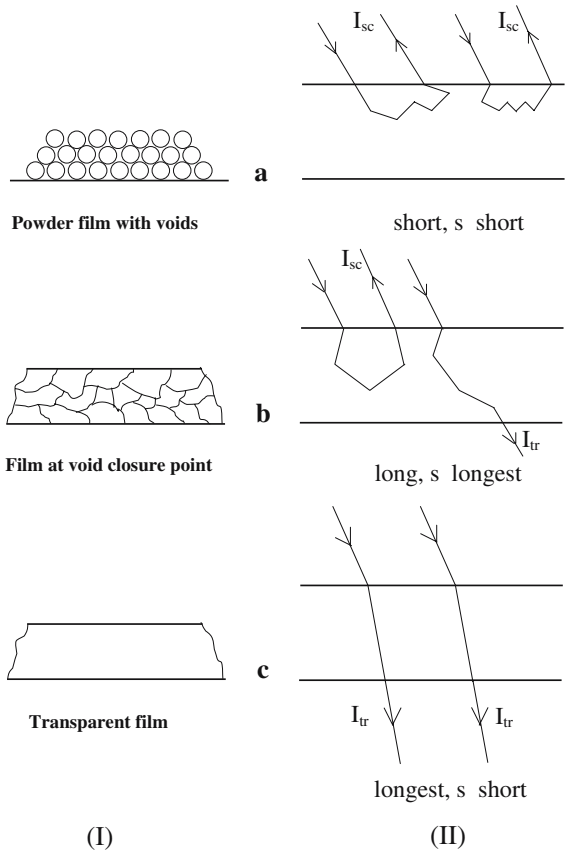

Fig. 2 Schematic illustrations of film formation from latex particles (*I*) and variation in mean free and optical paths (<l> and *s*) (*II*) during film formation. **a–c** Correspond to the film formation stages

The dependence of the viscosity of polymer melt on temperature is affected by the overcoming of the forces of macromolecular interaction which enables the segments of polymer chain to jump over from one equilibration position to another. This process happens at temperatures at which free volume becomes large enough and is connected with the overcoming of the potential barrier. The height of this barrier can be characterized by free energy of activation, ΔG, during viscous flow. Frenkel–Eyring [31] theory produces the following relation for the temperature dependence of viscosity:

$$\eta = \frac{N_0 h}{V}\exp\left(\Delta G/kT\right), \tag{3}$$

where N_0 is Avagadro's number, h is Planck' s constant, V is molar volume and k is Boltzmann constant. It is known that if $\Delta G = \Delta H - T\Delta S$, then Eq. 3 can be written as

$$\eta = A\exp\left(\Delta H/kT\right), \tag{4}$$

where ΔH is the activation energy of viscous flow, i.e. the amount of heat which must be given to one mole of

material for creating the act of a jump during viscous flow. ΔS is the entropy of activation of viscous flow. Here, A represents a constant for the related parameters. Combining Eqs. 2 and 4 the following useful equation is obtained:

$$t = -\frac{2A}{\gamma}\exp\left(\frac{\Delta H}{kT}\right)\int_{r_0}^{r}\rho(r)dr. \tag{5}$$

Equation 5 can be employed by assuming that the interparticle voids are in equal size, and number of voids stay constant during film formation (i.e. $\rho(r)\propto r^{-3}$). Then integration of Eq. 5 gives the relation

$$t = \frac{2AC}{\gamma}\exp\left(\frac{\Delta H}{kT}\right)\left(\frac{1}{r^2}-\frac{1}{r_0^2}\right), \tag{6}$$

where C is a constant related to relative density $\rho(r)$. As was stated before, a decrease in the void size r causes an increase in the mean free path <l> of a photon, which then results in an increase in I_{tr} and a decrease in I_{sc} intensities. Void radius r has a small size compared to the particle radius (367.6 nm). It is well known that scattering intensity increases with volume squared (the sixth power radius) of scattering object. If the assumption is made that I_{tr} is inversely proportional to the sixth power of void radius r, then Eq. 6 can be written as

$$t = \frac{2AC}{\gamma}\exp\left(\frac{\Delta H}{kT}\right)I_{tr}^{1/3}. \tag{7}$$

Here, r_0^{-2} is omitted from the relation because it is very small compared to r^{-2} values after void closure processes start. Equation 7 can be solved for I_{tr} to interpret the results in Fig. 1 as

$$I_{tr}(T) = S(t)\exp\left(-\frac{3\Delta H}{kT}\right), \tag{8}$$

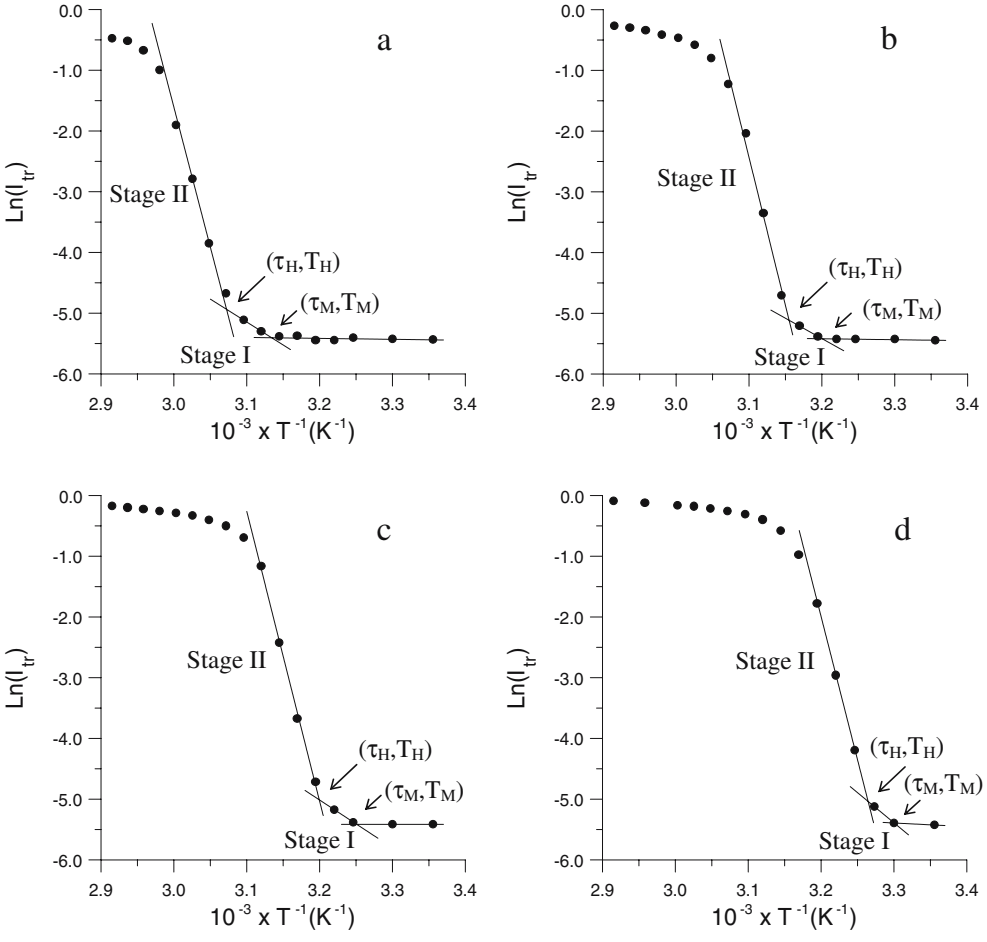

Fig. 3 Logarithmic plots of the data in Fig. 1 vs reverse of annealing temperature (T^{-1}) for the films annealed at **a** 1-, **b** 2.5-, **c** 5- and **d** 15-min time intervals. (τ_H,T_H) and (τ_M,T_M) pairs indicate healing and minimum film formation points, respectively

where $S(t) = \gamma t / 2AC^{1/2}$. For a given time the logarithmic form of Eq. 8 can be written as follows:

$$\ln I_{tr}(T) = \ln S(t) - \frac{3\Delta H}{kT}. \quad (9)$$

ln I_{tr} vs T^{-1} plots of the data in Fig. 1 are presented in Fig. 3 for the films annealed at (a) 1-, (b) 2.5-, (c) 5- and (d) 15-min time intervals. All the plots in Fig. 3 present two linearly increasing regions, where stages I and II represent void closure and interdiffusion processes, respectively, as predicted in Fig. 1. Intersections between the broken lines indicate the minimum film forming (τ_M,T_M) and healing points (τ_H,T_H). It can be seen that (τ_M,T_M) and (τ_H,T_H) points all shift to the right-hand side of the T^{-1} axis in Fig. 3, i.e. the left-hand side of the T axis in Fig. 1. This behaviour indicates that for short annealing times, films need higher minimum film forming (T_M) and healing temperatures (T_H). Figure 3 shows that the viscous flow process (stage I) has accomplished in a very narrow temperature region. Data in stage I in Fig. 3 are fitted to Eq. 9, and ΔH values are obtained from the slopes. The resultant ΔH values are listed in Table 2 for various time intervals. The averaged ΔH value was found to be 5.6 kcal/mol. Here, the ΔH values are found to be very close to carbon chain polymers in the literature (5–7 kcal/mol) [31].

Minimum film formation points (τ_M, T_M) can be treated with the Arrhenius plot as given below [22]:

$$\tau_M = B \exp(\Delta E_M / kT_M). \quad (10)$$

Here, ΔE_M presents the minimum film formation energy that the latex particles need to deform (τ_M,T_M) data are plotted in Fig. 4 for the films annealed at 1-, 2.5-, 5-, 10- and 15-min time intervals, where it is seen that as the minimum film formation time, τ_M is decreased, the MFFT, T_M increases by obeying Eq. 10. The logarithmic form of Eq. 10 is fitted to the data, and ΔE_M is produced from the slope of the straight line in Fig. 5 and found to be 32.5 kcal/mol. ΔE_M was found to be six times greater than ΔH, i.e. the energy need of polymeric system to perform the viscous flow process is much less than the energy needs to start the deformation of the particles.

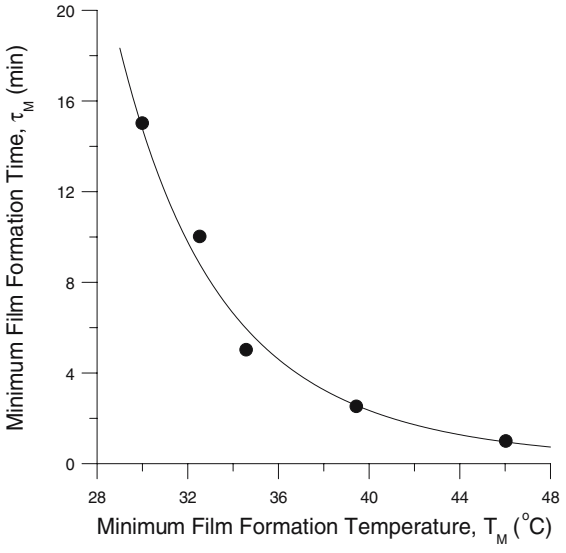

Fig. 4 Plot of minimum film formation time (τ_M) vs minimum film formation temperature (T_M) which obtained from the intersection of the first broken lines in Fig. 3

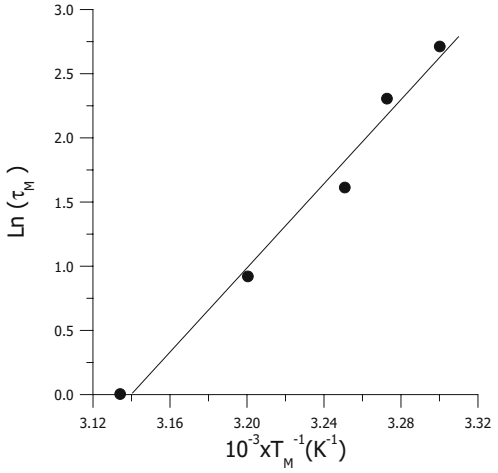

Fig. 5 Fit of the data in Fig. 4 to Eq. 10. Slope of the curve produces minimum film formation energy, ΔE_M

Healing at polymer–polymer interface

The healing (τ_H,T_H) pairs are plotted in Fig. 6, where it is seen that as τ_H is decreased, T_H increases to execute the healing process using minor chains during film formation.

Table 2 Viscous flow (ΔH) and backbone (ΔE_b) activation energies for different annealing times

	Annealing time (min)					Average
	1	2.5	5	10	15	
ΔH (kcal/mol)	5.0	4.4	5.2	7.0	6.6	5.6
ΔE_b (kcal/mol)	182.8	193.1	189.3	190.5	187.2	188.6

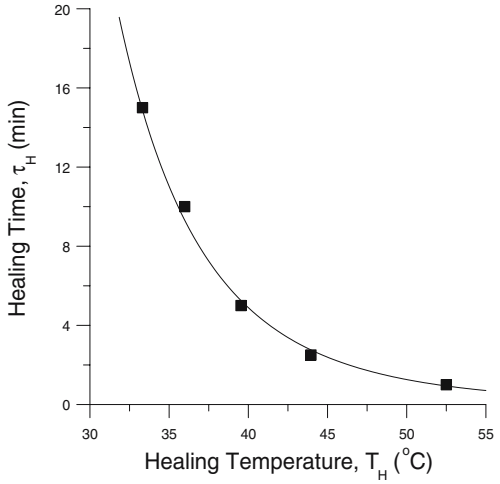

Fig. 6 Variation of healing points (τ_H,T_H) which obtained from the intersection of stage I–stage II lines in Fig. 3

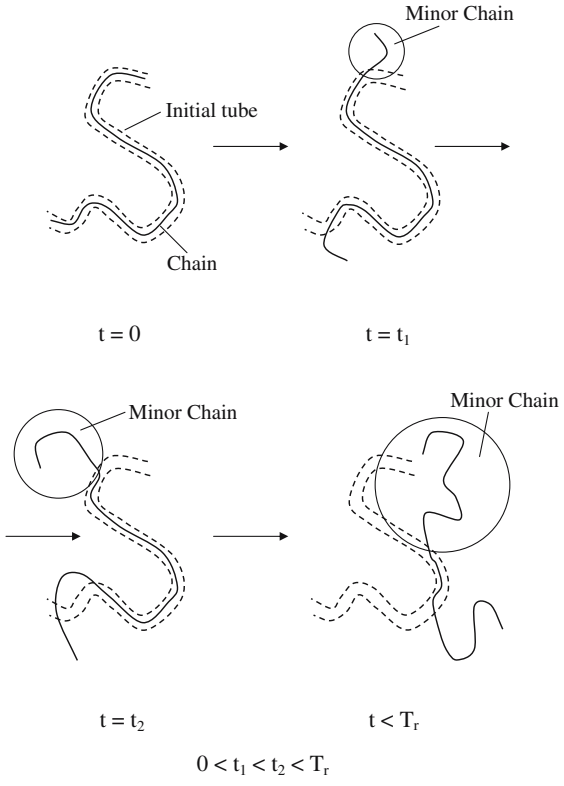

Fig. 7 Disengagement of a Gaussian chain from its initial tube in the reptation model, i.e. the growth of minor chain. T_r is the tube renewal time

Initially, below T_H, due to the sharp particle boundaries or voids between particles, light scatters from the film surface. Increasing of temperature causes wetting, which initiates segmental motion, and as a result, polymer chain segments move across the interface. Subsequently, more light can enter the latex film, and the transmission intensity increases.

To quantify the results in Fig. 6 we employed the minor chain model developed by Kim and Wool and Wool et al. [32, 33]. They used the reptation model of chain dynamics [15] where by a wriggling motion, a chain on average moves coherently back and forth along the centre line of the tube. The portions of a chain that are no longer in the initial tube increase with time and are referred to as a minor chain of length $l(t)$ (see Fig. 7). The conformations of the minor chains are always Gaussian. Kim and Wool [32] derived the average of the $l(t)$ values for times shorter than the tube renewal time (T_r) and found that

$$\langle l^2 \rangle = 2D\tau_H. \tag{11}$$

Here, the curvilinear diffusion coefficient, D, can be in the following form at T_H:

$$D = D_0 \exp\left(-\Delta E_H / kT_H\right), \tag{12}$$

where ΔE_H is the healing activation energy, which is the minimum energy required for a minor chain to move across to the junction surface, and k is the Boltzmann constant. If one assumes that $<l^2>$ values are identical at the healing temperatures of each separate set of experiments, then a very useful relation can be obtained from Eqs. 11 and 12:

$$\tau_H = B \exp\left(\Delta E_H / kT_H\right), \tag{13}$$

where $B = \langle l^2 \rangle / 2D_0$ is a constant. The fit of Eq. 13 to the data in Fig. 6 is shown in Fig. 8, where the slope of the straight line produced the ΔE_H value as 28.3 kcal/mol.

Chain reptation and interdiffusion

When film samples were annealed at elevated temperatures for various time intervals above the (τ_H,T_H), a continuous increase in I_{tr} intensities was observed until they become saturated (see Fig. 1). This further increase in I_{tr} (stage II) can be explained by the increase in transparency of latex film due to the disappearance of particle–particle boundaries known as interdiffusion. As the annealing temperature is increased, some of the polymer chains cross the junction surface and particle boundaries disappear, and as a result, the transmitted photon intensity I_{tr} increases. The increase in annealing temperature causes total transfer of polymer

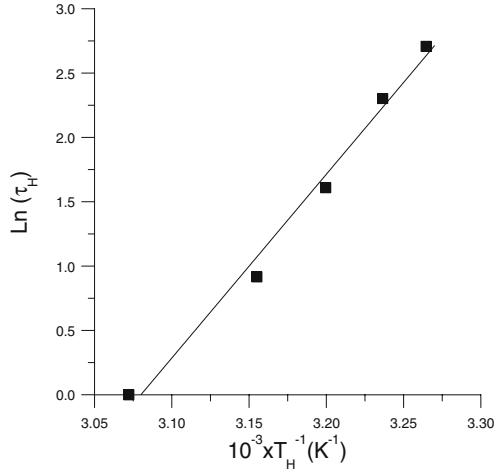

Fig. 8 Fit of the data in Fig. 6 to Eq. 13. Slope of the curve produces healing energy of minor chains, ΔE_{H}

chains across the boundary, which results in completely transparent film.

To quantify these results, the PT model [16] for the chain-crossing density can be employed. These authors used de Gennes's reptation model [15] to explain configurational relaxation at the polymer–polymer junction, where each polymer chain is considered to be confined to a tube in which it executes a random back and forth motion. A homopolymer chain with N freely jointed segments of length L was considered by PT, which moves back and forth by one segment with a frequency ν. In time the chain displaces down the tube by a number of segments (m). Here, $\nu/2$ is called the "diffusion coefficient" of m in one-dimensional motion. PT calculated the probability of the net displacement with m during time t in the range of $n-\Delta$ to $n-(\Delta+d\Delta)$ segments. A Gaussian probability density was obtained for small times and large N. The total "crossing density" $\sigma(t)$ (chains per unit area) at junction surface then was calculated from the contributions due to chains still retaining some portion of their initial tubes, $\sigma_1(t)$ plus a remainder, $\sigma_2(t)$. Here, the $\sigma_2(t)$ contribution (backbone motion) comes from chains which have relaxed at least once. In terms of reduced time $\tau = 2\nu t/N^2$ the total crossing density can be written as

$$\sigma(\tau)/\sigma(\infty) = 2\pi^{-1/2}\left\{\tau^{1/2} + 2\sum_{k=0}^{\infty}(-1)^n\left[\tau^{1/2}\exp\left(-k^2/\tau\right) - \pi^{-1/2}erfc\left(k/\tau^{1/2}\right)\right]\right\}. \quad (14)$$

For small τ values the summation term in the above equation is very small and can be neglected, which then results in

$$\sigma(\tau)/\sigma(\infty) = 2\pi^{-1/2}\tau^{1/2}. \quad (15)$$

This was predicted by de Gennes on the basis of scaling arguments. To compare our results with the crossing density of the PT model, the temperature dependence of $\sigma(\tau)/\sigma(\infty)$ can be modelled by taking into account the following Arrhenius relation for the linear diffusion coefficient:

$$\nu = \nu_0 \exp\left(-\Delta E_b/kT\right). \quad (16)$$

Here, ΔE_{b} is defined as the activation energy for the backbone of polymer chain. Combining Eqs. 15 and 16 a useful relation is obtained as

$$\frac{\sigma(T)}{\sigma(\infty)} = R\exp\left(-\Delta E_b/2kT\right), \quad (17)$$

where $R = \left(8\nu_0 t/\pi N^2\right)^{1/2}$ is a temperature-independent coefficient.

To explain the behaviour of I_{tr} at stage II in Fig. 1 it is assumed that I_{tr} is proportional to the crossing density $\sigma(T)$ at the interface; then, the phenomenological equation can be written as

$$\frac{I_{tr}(T)}{I_{tr}(\infty)} = R\exp\left(-\Delta E_b/2kT\right), \quad (18)$$

where the activation energies (ΔE_{b}) of backbone motion were produced by fitting the stage II data in Fig. 3 to logarithmic form of Eq. 18 and listed in Table 2. The averaged ΔE_{b} value is found as 188.6 kcal/mol. The backbone activation energy (ΔE_{b}) was found to be six times larger than the activation energy (ΔE_{H}) for the minor chains. It is quite reasonable to accept that small chain segment (minor chain) needs much less energy to execute its motion than the energy needed to cross the centre of mass of a chain through the particle–particle interfaces.

Conclusion

The results presented in this paper show that the film formation stages (void closure, healing and interdiffusion) and minimum film formation points that low-T_g PVAc latex particles can be observed from the data obtained by photon transmission. We fitted our UVV data to simple kinetic models and found the activation energies of each step of film formation. It was determined that the viscous flow and interdiffusion activation energies of PVAc latex are independent of the annealing time of latex films. As a result the photon transmission is a quite useful and inexpensive technique to observe the latex film formation process of low-T_g latex particles.

References

1. Keddie JL (1997) Mater Sci Eng 21:101
2. Eckersley ST, Rudin A (1990) JCT J Coat Technol 62:89
3. Joanicot M, Wong K, Maquet J, Chevalier Y, Pichot C, Graillat C, Linder P, Rios L, Cabane B (1990) Prog Colloid Polym Sci 81:175
4. Sperry PR, Snyder BS, O'Dowd ML, Lesko PM (1994) Langmuir 10:2619
5. Mackenzie JK, Shuttleworth R (1949) Proc Phys Soc 62:838
6. Mohammadi N, Klein A, Sperling LH (1993) Macromolecules 26:1019
7. Sambasivam M, Sperling LH, Klein A (1995) Macromolecules 28:152
8. Pekcan O, Arda E, Kesenci K, Piskin E (1998) J Appl Polym Sci 68:1257
9. Sambasivam M, Klein A, Sperling LH (1995) J Appl Polym Sci 58:357
10. Wang Y, Winnik MA (1993) J Phys Chem 97:2507
11. Canpolat M, Pekcan O (1995) Polymer 36:4433
12. Canpolat M, Pekcan O (1995) Polymer 36:2025
13. Pekcan O, Canpolat M (1996) J Appl Polym Sci 59:1699
14. Voyutskii SS (1963) Autohesion and adhesion of high polymers. Wiley, New York
15. de Gennes PG (1971) J Chem Phys 55:572
16. Prager S, Tirrell M (1981) J Chem Phys 75:5194
17. Wool RP, O'Connor KM (1981) J Appl Phys 52:5953
18. Vanderhoff JW (1970) Br Polym J 2:161
19. Distler D, Kanig G (1978) Colloid Polym Sci 256:1052
20. Hahn K, Ley G, Schuller H, Oberthur R (1988) Colloid Polym Sci 66:631
21. Oh JK, Tomba P, Ye X, Eley R, Rademacher J, Farwaha R, Winnik MA (2003) Macromolecules 36:5804
22. Ugur S, Elaissari A, Pekcan O (2003) J Colloid Interface Sci 263:674
23. Ugur S, Elaissari A, Pekcan O (2005) Polym Adv Technol 16:405
24. Arda E, Bulmus V, Piskin E, Pekcan O (1999) J Colloid Interface Sci 213:160
25. Arda E, Pekcan O (2001) Polymer 42:7419
26. Pekcan O, Arda E, Bulmus V, Piskin E (2000) J Appl Polym Sci 77:866
27. Pekcan O, Arda E (2001) Compos Interfaces 8:83
28. Arda E, Ozer F, Piskin E, Pekcan O (2001) J Colloid Interface Sci 233:271
29. Keddie JL, Meredith P, Jones RAL, Ronald AM (1996) In: Provder T, Winnik MA, Urban MW (eds) Film formation in waterborne coatings. Proc ACS Symp Ser 648, Washington, DC, pp 332–348
30. Mc Kenna GB (1989) In: Booth C, Price C (eds) Comprehensive polymer science, vol 2. Pergamon, Oxford
31. Tager A (1978) Physical chemistry of polymers. MIR, Moscow
32. Kim YH, Wool RP (1983) Macromolecules 16:1115
33. Wool RP, Yuan BL, Mc Garel OJ (1989) Polym Eng Sci 29:1340